Asymmetry of a complex gap near the Fermi level, determined from measurements of the thermopower in La$_{1-x}$Ca$_x$Mn$_{1-y}$Fe$_y$O$_3$

Asymmetry of a complex gap near the Fermi level, determined from measurements of the thermopower in $La_{1-x}Ca_xMn_{1-y}Fe_yO_3$

R Laiho[1], **K G Lisunov**[1,2], **E Lähderanta**[1], **V N Stamov**[1,2], **V S Zakhvalinskii**[1,2], **A I Kurbakov**[3] **and A E Sokolov**[3]

[1] Wihuri Physical Laboratory, Department of Physics, University of Turku, FIN-20014, Turku, Finland
[2] Institute of Applied Physics, Academiei Street 5, MD-2028 Kishinev, Moldova
[3] St Petersburg Nuclear Physics Institute, 188 300 Gatchina, Leningrad District, Russia

Abstract
The thermopower, S, of $La_{0.7}Ca_{0.3}Mn_{1-y}Fe_yO_3$ ($y = 0$–0.09), measured for $T = 25$–310 K and magnetic fields of $B = 0$–10 T, exhibits strong sensitivity to doping with Fe. The weak increase of S observed in the undoped material with lowering temperature is enhanced considerably in the sample with $y = 0.03$ until a steep decrease takes place in the vicinity of the paramagnetic–ferromagnetic transition temperature, T_C. S increases with further growth of y and its maximum follows the decrease of T_C from 228 K at $y = 0.03$ to 119 K at $y = 0.09$. Application of a magnetic field reduces S strongly. The experimental data are analysed quantitatively with a percolation model using results of our recent investigations of the Shklovskii–Efros-like variable-range hopping conductivity in the same set of $La_{1-x}Ca_xMn_{1-y}Fe_yO_3$ samples with evidence for a soft Coulomb gap and a rigid gap in the density of states near the Fermi level (Laiho *et al* 2002 *J. Phys.: Condens. Matter* **14** 8043). In the paramagnetic insulating phase the temperature dependence of S is determined by competing contributions from two types of asymmetry of the gap: a small shift of its centre with respect to the Fermi level and cubic non-parabolicity. Numerical values of the shift and the cubic asymmetry terms are determined.

(Some figures in this article are in colour only in the electronic version)

1. Introduction

$La_{1-x}Ca_xMn_{1-y}Fe_yO_3$, in brief LCMFO, is obtained by substitution of Fe for Mn in the hole-doped colossal magnetoresistance (CMR) material $La_{1-x}Ca_xMnO_3$ (LCMO) [1]. Besides the huge drop of the resistivity, ρ, in a magnetic field, B, near the paramagnetic (PM) to ferromagnetic (FM) transition temperature T_C, a series of new interesting phenomena are

observed in LCMFO. Among them is the strong influence of doping with Fe on the magnetic properties, including a large decrease of T_C [2, 3], enhancement of the magnetic irreversibility and the relaxation of the thermoremanent magnetization [4] and increase of ρ by several orders of magnitude [5, 6]. At a low doping level direct replacement of Mn^{3+} by Fe^{3+} should take place [7], forming Fe^{3+}–Mn^{4+} pairs [3] which do not support the double-exchange interaction responsible for the ferromagnetism in the manganese perovskites [8]. The relative concentration of the holes, $c \approx x$, introduced by substitution of Ca^{2+} for La^{3+} is diminished to $c \approx x - y$ leading to decrease of T_C [9]. Besides the Jahn–Teller (JT) effect [10], the lattice disorder induced by doping with Fe is another important reason for localization of the holes [11, 12] and decrease of T_C with increasing y [4]. The disorder and random breaking of the double-exchange interactions by the Fe^{3+}–Mn^{4+} pairs are responsible for transformation of the weakly frustrated FM phase to the mixed FM and glassy state in LCMFO [4].

Investigations of the variable-range hopping (VRH) conductivity in LCMFO [12] confirmed the complex density of localized states, $g(\varepsilon)$, observed by scanning–tunnelling spectroscopy in a LCMO film with $x = 0.2$ [13], comprising a soft gap, Δ, or parabolic dependence of $g(\varepsilon)$ on the energy inside an interval of $\Delta \sim 0.4$ eV around the Fermi level, μ, and a rigid gap at $g(\varepsilon) = 0$ with the maximum width $2\delta = 0.215$ eV. Both δ and $g(\varepsilon)$ outside the soft gap were found to depend on T. The soft gap was attributed to long-range Coulomb interactions between the localized electrons and the rigid gap to the Jahn–Teller effect [13].

As demonstrated in [12], the resistivity of LCMFO with $x = 0.3$ and $y = 0$–0.09 satisfies in the PM phase the Shklovskii–Efros (SE) law [14], $\rho(T) = \rho_0 \exp[(T_0/T)^{1/2}]$, where the characteristic temperature T_0 is independent of B and T at temperatures well above T_C but becomes a function of B and T near T_C. The SE VRH mechanism is connected directly to the existence of the soft Coulomb gap Δ around μ [14]. In addition, the values and the dependence of the rigid gap δ on B and T were also extracted from the analysis of the VRH conductivity in the magnetic field [12]. Near the onset temperature of the VRH conductivity, T_v, δ is independent of B but depends on T as $\delta(T) \approx \delta_v(T/T_v)^{1/2}$, where δ_v is a constant. As T approaches T_C, deviations of $\delta(T)$ from the square root dependence, increasing with B, are observed [12].

In this paper we report experimental results on the temperature and magnetic field dependence of the thermopower, S, in $La_{0.7}Ca_{0.3}Mn_{1-y}Fe_yO_3$ using the same samples as in the conductivity measurements [12]. Analysis of the dependence of S on B and T yields new information about the structure of the density of states near the Fermi level in this compound.

2. Experimental details

LCMFO with $x = 0.3$ and $y = 0, 0.03, 0.07, 0.09$ (sample Nos 3–0, 3–3, 3–7 and 3–9, respectively) was synthesized with the standard ceramic procedure by heating stoichiometric mixtures of La_2O_3, $CaCO_3$, Mn_2O_3 and Fe_2O_3 in air at 1320 °C, at first for 15 h, then for 5 and 15 h and finally at 1375 °C for 22 h, with intermediate grindings. Detailed neutron diffraction investigations for $T = 20$–300 K on the samples 3–0, 3–3 and 3–9 revealed an orthorhombic structure with the space group $Pnma$. The values of the lattice parameters a, b and c, as well as the coordinates of the La (Ca), Mn (Fe) and O atoms are in a good agreement with the earlier data obtained by neutron powder diffraction measurements on LCMFO (see e.g. [15]). Magnetization $M(T)$ was measured with an rf SQUID magnetometer after cooling the sample from the room temperature down to 5 K in a field of $B = 2$ G. The values of S were determined with the standard dc technique in a chamber where the temperature of the sample could be regulated and a temperature gradient could be created by two independent heaters fixed at its ends. This allowed us to control the quality of the contacts and to remove the error connected
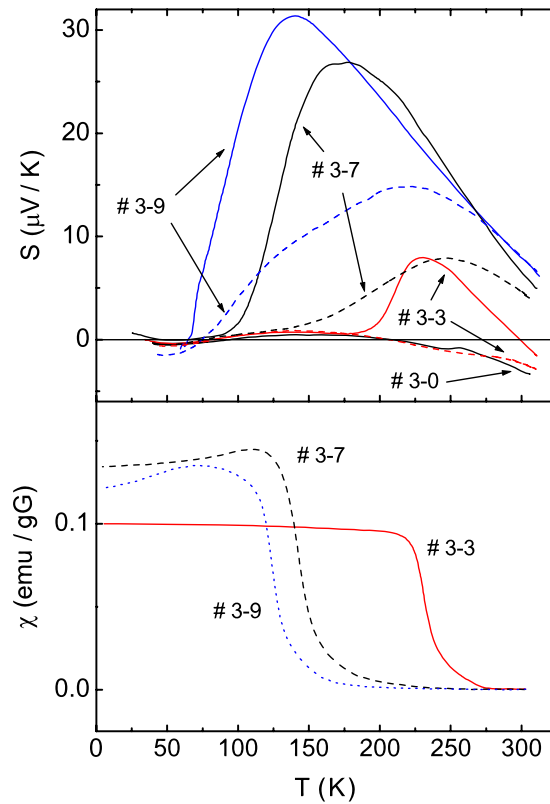
Figure 1. Upper panel: the temperature dependence of S in $La_{0.7}Ca_{0.3}Mn_{1-y}Fe_yO_3$ with $y = 0$, 0.03, 0.07 and 0.09 in the fields of $B = 0$ (solid curves) and 10 T (dashed curves). Lower panel: the temperature dependence of the susceptibility $\chi = M/B$ measured in the field of $B = 2$ G.

to the voltmeter bias by changing the direction of the temperature gradient. The data were calibrated by measuring the thermo-emf of LCMFO against a Cu standard sample.

3. Results and discussion

As can be seen from figure 1 (upper panel) the temperature dependence of S is weak in No 3–0 and above $\sim$200 K its sign is negative. A strong increase of S, accompanied by change of the sign, is observed in the PM phase when y is increased. The $S(T)$ curve has a maximum at a temperature T_m near the PM–FM transition shown by the magnetic susceptibility data in the lower panel of figure 1 (the values of T_C for samples 3–3 to 3–9 are collected in table 1). The value of S decreases steeply with lowering temperature below T_m, which decreases similarly to T_C when y is increased.

Application of a magnetic field strongly decreases the value of S and shifts T_m towards higher temperatures (see also figure 2). Generally, the functions $S(T)$ and $S(B)$ shown in figures 1 and 2 resemble those observed in many other manganese perovskites, e.g. $La_{1-x}Ca_xMnO_{3+\delta}$ [16], $La_{1-x}Sr_xMnO_3$ [17] and LCMFO with $x = 0.35$ and $y = 0$–0.07 [18]. It should be mentioned also that the shift of T_m is enhanced and the sensitivity of S to B is weakened when y is increased from 0.03 to 0.09. Comparing the data on $S(T)$ and $\rho(T)$ (see figure 1(a) of [12]) of LCMFO in a magnetic field a large difference is observed
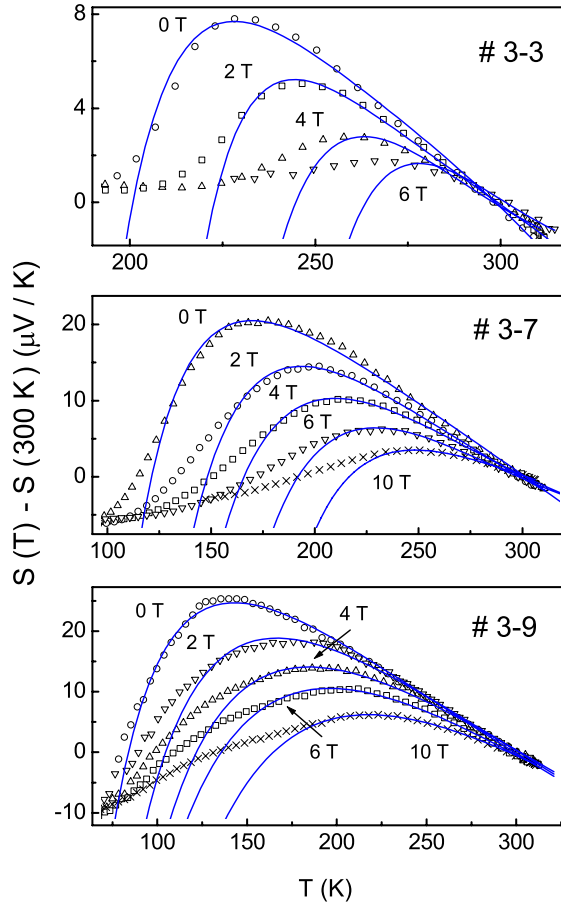
Figure 2. The dependence of $S(T) - S$ (300 K) on temperature. The solid curves are fits to the experimental data using equations (5)–(7).

Table 1. The values of the relative concentration of Fe y, the PM–FM transition temperature T_C, the temperature of the onset of VRH T_v [12], the high-temperature value of the characteristic VRH temperature T_0^* [12], the width of the Coulomb gap Δ [12], the width of the rigid gap $\delta_v = \delta(T_v)$ [12], the coefficient of the cubic asymmetry α, the parameter ξ and the shift of the gap γ.

Sample Nos	y	T_C (K)	T_v (K)	T_0^* (10^4 K)	Δ (eV)	δ_v (eV)	α (eV^{-1})	ξ	γ (meV)
3–3	0.03	228	330	7.7	0.43	0.16	-0.99 ± 0.06	0.73 ± 0.02	8.2 ± 0.5
3–7	0.07	139	310	7.3	0.40	0.14	-1.06 ± 0.07	0.72 ± 0.02	8.4 ± 0.6
3–9	0.09	119	316	7.7	0.41	0.12	-0.99 ± 0.05	0.73 ± 0.02	8.8 ± 0.5

between T_m and the temperature of the resistivity maximum T_m' for $y = 0.07$ and 0.09. The position of T_m' is less influenced by B than that of T_m. In addition, the drop of ρ in the field is enhanced considerably when y is increased [12]. Therefore, the thermopower does not directly match the behaviour of the resistivity. On the other hand, the field dependence of the ratio $T_0(T)/T_0^*$ (T_0^* is the value of T_0 well above T_C) shown in figure 3 and of the values of $\delta(T)$
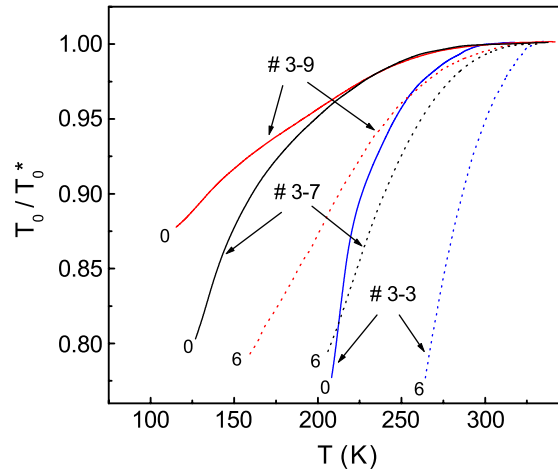
Figure 3. The temperature dependence of T_0/T_0^* in the fields $B = 0$ (solid curves) and 6 T (dotted curves).

(see figure 8 of [12]) obtained from the analysis of $\rho(T, B)$ [12] becomes smaller when y is increased, similar to the behaviour of $S(T)$ in figures 1 and 2.

Zvyagin [19] has proposed a model of S in the VRH regime, based on percolation over the Miller–Abrahams network [20], suggesting that a major contribution to S comes from the current flowing in the backbone cluster. The latter is part of a critical subnetwork consisting of the chains of bonds (macrobonds) corresponding to optimal hopping paths. Within this approach S satisfies the expression [19]

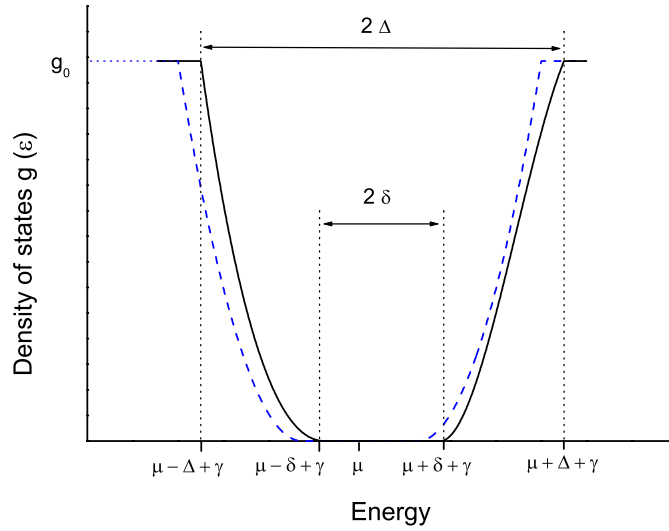$$S = \frac{1}{eT}\langle \varepsilon - \mu \rangle \tag{1}$$

where $\langle \varepsilon - \mu \rangle$ is the average energy with respect to μ of the hopping carriers contributing to S. Generally, the value of S given by equation (1) is determined by asymmetries of the density of states and of the transition rates involved in intrasite Hubbard correlation effects [19].

For a repulsive Hubbard interaction, $K > 0$, the average occupation number of a site was found to be a two-step function, $f(\varepsilon) = 1$ at $\mu - K < \varepsilon < \mu$ and $f(\varepsilon) = 2$ at $\varepsilon < \mu - K$, with small broadening of the steps induced by the temperature and the distribution of the Hubbard correlation energies K [19]. For the hydrogen-like wavefunctions of the localized carriers [21] $K = 5e^2/(8\kappa a_{loc})$, where κ is the dielectric constant and a_{loc} is the localization radius of the charge carriers. For $\kappa \approx 3.5$ and $a_{loc} \approx 3$ Å [12] we find $K \approx 0.88$ eV which is more than twice the value of Δ in table 1. This means that double-occupied sites in LCMFO can exist only outside the Coulomb gap and the contribution to the thermopower from the Hubbard correlations for $T < T_v$, where T_v is the onset temperature of the VRH conductivity over the states inside the gap (table 1), can be neglected. In this case equation (1) can be written as

$$S = \frac{1}{eT}\frac{Q_1}{Q_0} \tag{1'}$$

where

$$Q_k = \int_{\mu-\varepsilon_m}^{\mu+\varepsilon_m} (\varepsilon - \mu)^k g(\varepsilon) p(\varepsilon)\, d\varepsilon, \qquad k = 0, 1. \tag{2}$$

Figure 4. The density of states $g(\varepsilon)$ given by equation (3) in the region of the Coulomb gap (Δ) and the rigid gap (δ) (solid curve) with the centre shifted from the Fermi level μ by the value of γ (schematic). The dashed curve represents the DOS evaluated with equation (3) at $\alpha = \gamma = 0$.

Here $\varepsilon_{\mathrm{m}} = k(T_0 T)^{1/2}$ is the maximum energy of the hopping carriers and the probability for a site with an energy ε to belong to the backbone cluster is approximated as $p(\varepsilon) \approx \theta(\xi \varepsilon_{\mathrm{m}} - |\varepsilon - \mu|)$, where $\theta(x)$ is the Heaviside step function and ξ is a constant [19].

It has been proposed that the asymmetry of the density of states is determined in the region of the Coulomb gap by a cubic term [19], $g(\varepsilon) = C_0 \varepsilon^2 (1 + \alpha \varepsilon)$, where $C_0 = \alpha_3 \kappa^3 / e^6$ and $\alpha_3 = 3/\pi$ [14]. Another type of asymmetry can arise from a small shift, γ, of the centre of the gap with respect to μ. Therefore, we generalize the symmetrical $g(\varepsilon)$ function applied to interpret the resistivity [12] to

$$g(\varepsilon) = \begin{cases} g_0, & \varepsilon < \mu - \Delta + \gamma, \\ C_1(\varepsilon - \mu + \delta - \gamma)^2[1 + \alpha(\varepsilon - \mu + \delta - \gamma)], & \mu - \Delta + \gamma < \varepsilon < \mu - \delta + \gamma, \\ 0, & \mu - \delta + \gamma < \varepsilon < \mu + \delta + \gamma, \\ C_2(\varepsilon - \mu - \delta - \gamma)^2[1 + \alpha(\varepsilon - \mu - \delta - \gamma)], & \mu + \delta + \gamma < \varepsilon < \mu + \Delta + \gamma, \\ g_0, & \varepsilon > \mu + \Delta + \gamma, \end{cases}$$

(3)

where $g_0 = C_0 D^2$, $C_1 = C_0(1 + \alpha D)^{-1}$, $C_2 = C_0(1 - \alpha D)^{-1}$ and $D = \Delta - \delta$. The asymmetric $g(\varepsilon)$ function given by equation (3) is shown schematically in figure 4 (the solid curve) along with the symmetrical form (the dashed curve) [12] obtained from equation (3) with $\alpha = \gamma = 0$.

For the case of symmetrical density of states the characteristic VRH temperature, which determines all features of the resistivity in the VRH regime, is given by the equation [12]

$$T_0 = \left(\frac{\delta}{2k\sqrt{T}} + \sqrt{\frac{\delta^2}{4k^2 T} + T_{0SE}} \right)^2,$$

(4)

where $T_{0SE} = \beta e^2/(\kappa k a_{\mathrm{loc}})$ and $\beta = 2.8$ is a constant [14]. It can be shown in the way used to obtain equation (4) [12] that T_0, in the case of the asymmetrical density of states given by equation (3), satisfies equation (4) in the zeroth approximation over the small parameter $\gamma/(\xi \varepsilon_{\mathrm{m}} - \delta)$ with T_{0SE} replaced by $T_{SE} = \beta' e^2/(\kappa k a_{\mathrm{loc}})$, where $\beta' =$

$\beta[1 - (\alpha D)^2]^{1/3}\{1 - (1/4)\alpha^2 D(\varepsilon_m - \delta)/[1 - (\alpha D)^2]\}^{-1/3}$. Because $\varepsilon_m - \delta < D$, the influence of the asymmetry of the $g(\varepsilon)$ function on the resistivity can be neglected provided that $(\alpha D)^2 \ll 1$.

The expression of S, obtained in the first nonzero approximation over $\gamma/(\xi\varepsilon_m - \delta)$ with equations (1')–(3), can be presented in the form

$$S(T) = S_1(T) + S_2(T) \tag{5}$$

where the term

$$S_1(T) = \frac{4\gamma(2\xi\varepsilon_m + \delta)}{T(4 - 3\alpha D)} \tag{6}$$

is determined mainly by the shift of the gap and

$$S_2(T) = \frac{\alpha[3(\xi\varepsilon_m - \delta)(4\xi\varepsilon_m + \delta) - 5D(3\xi\varepsilon_m + \delta)]}{5T(4 - 3\alpha D)} \tag{7}$$

is determined by the cubic asymmetry term in the function $g(\varepsilon)$.

It has been proposed that the complete expression for S in the hole-doped manganese perovskites should also contain a spin term [22, 23], associated not with the asymmetry of $g(\varepsilon)$ but with the configurational entropy for a spin-3/2 hole moving in the spin-2 background. In the PM phase this term is considered to be temperature independent and therefore can be excluded from the analysis by subtraction.

To analyse the plots of $S(T) - S$ (300 K) in figure 2 we use the temperature dependences of T_0/T_0^* and δ obtained from the analysis of the resistivity (see figures 3 and 8 of [12]) or evaluated using the method proposed in [12] (figure 3) and the values of T_0^* and Δ in table 1 [12]. The plots of $S(T) - S$ (300 K) are fitted with equations (5)–(7) to obtain the best agreement for the temperatures where the functions of $T_0(T)/T^*$ and $\delta(T)$ are appropriate (figure 3), treating the parameters α, ξ and γ as independent of T. Some details of the fitting procedure are presented in figure 5. In the upper panel are shown the contributions from $S_1(T) - S_1$ (300 K) and $S_2(T) - S_2$ (300 K), and in the lower panel the changes of the calculated $S(T) - S$ (300 K) curve caused by $\pm 5\%$ variation of one of the parameters, ξ, γ and α, while the other two remain constant. Sufficient sensitivity of the fitting procedure to variations of all the fitting parameters is found.

The plots obtained in the way described above are shown by the solid curves in figure 2. At $B = 0$ they reproduce explicitly the experimental data over the whole temperature interval of the PM phase of LCMFO, including in the close proximity of T_C. The drop of the resistivity below T_C (see figure 1(a) of [12]) is due to the onset of the FM metallic phase, which is shifted to higher temperatures as B is increased [24, 25]. Therefore, the onset of the deviations of the calculated curves from the experimental plots of $S(T)$ at higher temperatures with increasing B can be explained by reduction of the interval of the applicability of equations (5)–(7). Close values of the parameters ξ, α and γ are found in different samples (see table 1) and they do not demonstrate any systematic dependence on B. The value of ξ for a density of states function varying slowly with energy (leading to the Mott VRH conductivity with $\ln\rho \sim T^{-1/4}$) [26] was estimated to be two times smaller, $\xi \approx 0.35$ [19, 27]. Therefore, the enhanced value of ξ should be attributed to the strong variation of $g(\varepsilon)$ inside the gap (figure 4). At the same time, one can also find that the values of $\gamma/(\xi\varepsilon_m - \delta) \sim 0.1$ and $(\alpha D)^2 \sim 0.1$ are small enough to satisfy the conditions of applicability of $g(\varepsilon)$ given by equation (3) to both the resistivity and the thermopower. Finally, the density of states evaluated with equation (4) for one of the samples investigated is shown in figure 6 (note that in this figure the energies are measured from μ). Both types of asymmetry of $g(\varepsilon)$ are small and the contribution from the cubic term is slightly enhanced as T is decreased.
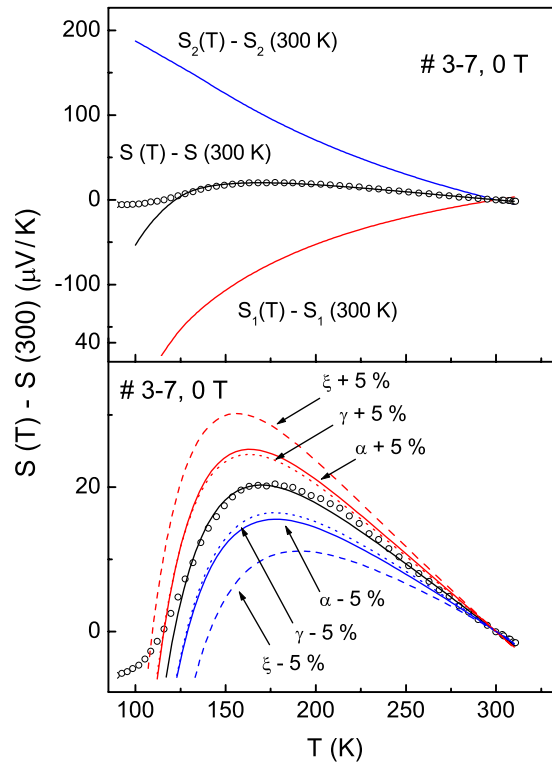
Figure 5. The dependence of $S(T) - S$ (300 K) on temperature for No 3–7 at $B = 0$. Upper panel: the contributions of $S_1(T) - S_1$ (300 K) and $S_2(T) - S_2$ (300 K) to $S(T) - S$ (300 K). Lower panel: the sensitivity of the parameters ξ, γ and α to the fitting of the temperature dependence of $S(T) - S$ (300 K).
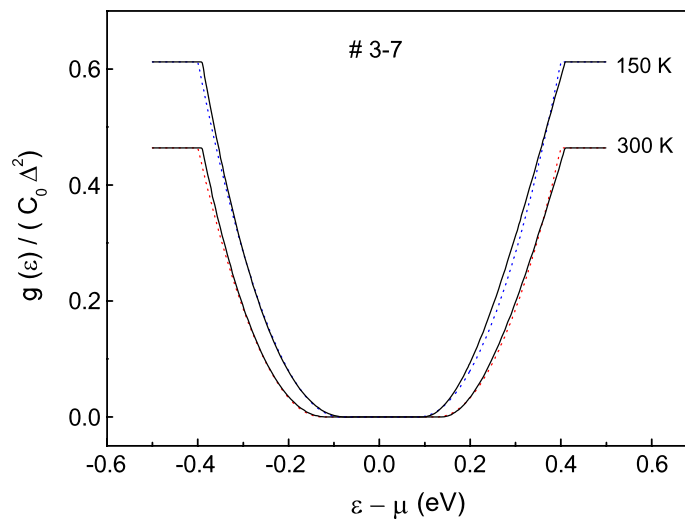
Figure 6. The density of states in the region of the Coulomb gap and the rigid gap evaluated with equation (3) using the values of $\alpha = -1.06$ eV^{-1} and $\gamma = 8.4$ meV obtained in this work (table 1). The dashed curve represents the DOS evaluated with equation (3) at $\alpha = \gamma = 0$.

Hence, the magnetic field and temperature dependences of S in the PM insulating phase of LCMFO can be explained by competing contributions from the two types of gap asymmetry, both depending on B and T via the corresponding dependences of the characteristic VRH temperature and the rigid gap. However, this does not provide the final solution of the problem but readdresses it to the origin of the sensitivity of T_0 and δ to the temperature and the magnetic field. A possible reason for both may be the reduction of the JT distortions when approaching the FM metallic phase, as observed in high-resolution neutron powder diffraction measurements on $La_{0.52}Y_{0.15}Ca_{0.33}MnO_3$ [28]. Indeed, from the analysis of the resistivity it has been concluded that a conventional metal–insulator transition (MIT), similar to that in doped semiconductors [29], and determined by the divergence of the localization radius, does not take place in LCMFO [11, 12], since both a_{loc} and T_{0SE} are finite down to $T'_m < T_C$. On the other hand, the reduction of the JT distortions leads to decrease of the depth of the polaron potential well, decreasing the carrier localization and increasing a_{loc}. Therefore, taking into account equation (4), T_0 would be diminished even at a constant δ. The values of $\delta_v = \delta(T_v)$ (table 1) were found to be about the half of the polaron binding energy in LCMO, $E_b/2 \sim E_{act} \approx 0.08$–$0.14$ eV, where E_{act} is the activation energy of the adiabatic small-polaron nearest-neighbour hopping conductivity in LCMO for $T \approx 300$–1200 K [30]. To hop from one site to another the carrier should annihilate polarization on the initial site and create it on the final site. This requires a minimum energy available for the hopping leading to the appearance of the rigid gap in the density of states around μ if the major contribution to the localization of the carrier is due to the JT distortions, whereas that from the lattice disorder is much smaller. On the other hand, the disorder in LCMFO increasing with y [4, 11, 12] leads to a finite distribution of the carrier potential energy and, as a result, to diminution of the gap by the value of the width of this distribution. Therefore, the width of the rigid gap is diminished when y is increased, as can be clearly seen from table 1 (see also figure 8 of [12]). Associated with the polaron binding energy, δ is sensitive to reduction of the JT distortions, which can explain its decrease with lowering temperature. The sensitivity of T_0 and δ to magnetic field, in turn, can be ascribed to the magnetic contribution in formation of the polaron [31].

4. Conclusions

The thermopower of $La_{0.7}Ca_{0.3}Mn_{1-y}Fe_yO$ with $y = 0, 0.03, 0.07$ and 0.09 is investigated at temperatures of 25–310 K and in magnetic fields of 0–10 T. The analysis of the experimental data has been done with the Zvyagin model of the thermopower in the region of variable-range hopping conductivity [19]. It is shown that in the temperature interval of the VRH conductivity regime in the paramagnetic insulating phase the thermopower can be interpreted in terms of the competing contributions of shifting the centre of the gap in the density of the localized states and the cubic non-parabolicity of the gap, having opposite signs. The dependence of S on temperature and magnetic field is governed by the corresponding dependences of the characteristic VRH temperature T_0 and the width of the rigid gap δ. The value of the shift of the gap and the contribution of the cubic term to the energy dependence of the density of the states obtained in this work, together with the magnetic field and temperature dependences of T_0 and δ found from the analysis of the resistivity in the same material [12], provide an explicit quantitative agreement with the experimental data.

Acknowledgments

References

[1] Schiffer P, Ramirez A P, Bao W and Cheong S-W 1995 *Phys. Rev. Lett.* **75** 3336
[2] Ahn K H, Wu X W, Liu K and Chien C L 1996 *Phys. Rev.* B **54** 15299
[3] Ahn K H, Wu X W, Liu K and Chien C L 1997 *J. Appl. Phys.* **81** 5505
[4] Laiho R, Lisunov K G, Lähderanta E, Salminen J and Zakhvalinskii V S 2002 *J. Magn. Magn. Mater.* **250** 267
[5] Hasanain S K, Nadeem M, Shah W H, Akhtar M J and Hasan M M 2000 *J. Phys.: Condens. Matter* **12** 9007
[6] Ogale S B, Shreekala R, Bathe R, Date S K, Patil S I, Hannoyer B, Petit F and Marest G 1998 *Phys. Rev.* B **57** 7841
[7] Jonker G H 1954 *Physica* **20** 1118
[8] de Gennes P-G 1960 *Phys. Rev.* **118** 141
[9] Varma C M 1996 *Phys. Rev.* B **54** 7328
[10] Millis A J, Littlewood P B and Shraiman B I 1995 *Phys. Rev. Lett.* **74** 5144
[11] Laiho R, Lähderanta E, Salminen J, Lisunov K G, Zakhvalinskii V S, Safontchik M O, Shakhov M A and Shubnikov M L 2002 *J. Appl. Phys.* **91** 7400
[12] Laiho R, Lisunov K G, Lähderanta E, Petrenko P A, Salminen J, Shakhov M A, Safontchik M O, Stamov V S, Shubnikov M V and Zakhvalinskii V S 2002 *J. Phys.: Condens. Matter* **14** 8043
[13] Biswas A, Elizabeth S, Raychaudhuri A K and Bhat H L 1999 *Phys. Rev.* B **59** 5368
[14] Shklovskii B I and Efros A L 1984 *Electronic Properties of Doped Semiconductors* (Berlin: Springer)
[15] Simopoulos A, Pissas M, Kallias G, Devlin E, Moutis N, Panagiotopoulos I, Niarchos D, Christides C and Sonntag R 1999 *Phys. Rev.* B **59** 1263
[16] Vergara J, Ortega-Hertogs R J, Madurga V, Sapira E, El-Fadli Z, Martinez E and Beltran A 1999 *Phys. Rev.* B **60** 1127
[17] Uhlenbruck S, Buchler B, Gross K, Freimuth A, Guevara A and Revcolevschi A 1998 *Phys. Rev.* B **57** R5571
[18] Aslam A, Hasanain S K, Zubair M, Akhtar M J and Nadeem M 2002 *J. Phys.: Condens. Matter* **14** 10305
[19] Zvyagin I P 1991 *Hopping Transport in Solids* ed M Pollak and B Shklovskii (Amsterdam: North-Holland) p 143
[20] Miller A and Abrahams E 1960 *Phys. Rev.* **120** 745
[21] Mott N F and Davies E A 1979 *Electron Processes in Non-Crystalline Materials* (Oxford: Clarendon) p 124
[22] Jaime M, Salamon M B, Rubinstein M, Treece R E, Horwitz J and Chrisen D B 1996 *Phys. Rev.* B **54** 11914
[23] Hunndly M F and Neumeier J J 1997 *Phys. Rev.* B **55** 11511
[24] Von Helmolt R, Wecker J, Holzapfel B, Schulz L and Sammer K 1993 *Phys. Rev. Lett.* **71** 2331
[25] Ramirez A P 1997 *J. Phys.: Condens. Matter* **9** 8171
[26] Mott N F 1990 *Metal–Insulator Transitions* (London: Taylor and Francis)
[27] Zvyagin I P 1973 *Phys. Status Solidi* b **58** 443
[28] Garcia-Munoz J L, Suaaidi M, Fontcuberta J and Rodriguez-Carvajal J 1997 *Phys. Rev.* B **55** 34
[29] Castner T G 1991 *Hopping Transport in Solids* ed M Pollak and B Shklovskii (Amsterdam: North-Holland) p 3
[30] Worledge D C, Snyder G J, Beasley M R, Geballe T H, Hiskes R and DiCarolis S 1996 *J. Appl. Phys.* **80** 5158
[31] De Teresa J M, Ibarra M R, Blasco J, Garcia J, Marquina C, Algarabel P A, Arnold Z, Kamenev K, Ritter C and von Helmolt R 1996 *Phys. Rev.* B **54** 1187